

## Advanced Material Models for Stamping of AW 5754 Aluminum Alloy

J. Slota<sup>1</sup> and M. Šiser<sup>2</sup>

Technical University, Košice, Slovakia

<sup>1</sup> jan.slota@tuke.sk

<sup>2</sup> marek.siser@tuke.sk

*Predictions by numerical simulations are strongly influenced by availability and reliability of input data. In the most used computational models, the material behavior during deformation is described only by static tensile test in combination with Lankford coefficients of anisotropy. However, for some specific materials like highly anisotropic aluminum alloys, such description of material behavior is insufficient and, in many cases, the calculated results are not in good agreement with the measured ones. In this paper, the implementation of advanced material model for deep-drawing process to explicit FE code and the procedure of measurement of the most important input material data for calculations on the aluminum alloy AW 5754 are discussed. Results of the numerical simulation are compared with the experimental ones and exhibit a close correlation.*

**Keywords:** aluminum alloy, anisotropic yield criterion, numerical simulation, stamping.

**Introduction.** Nowadays, there is a great demand for high-quality FE models within the numerical simulations, because significant part of the production problems can be eliminated in the preproduction phase using the finite element analysis (FEA). For precise prediction of the true forming process, the selection and accuracy of material input data are very important. Most of phenomena observed in sheet metal forming like hardening, anisotropy, failure and fracture occur simultaneously and may deeply affect the behavior of the material due to the important changes they cause in its physical and mechanical properties, such as formability, hardness, strength, springback and others [1]. Numerical simulation of the sheet metal forming processes requires the implementation of several types of models. The first type comprises the flow behavior, i.e., hardening models and yield criteria of the sheet metal, while others predict the forming limits under specific processing conditions. Recently, a lot of computational models within the metal forming regard yield criteria were developed [2–4], one of these being the anisotropic yield criterion proposed by Vegter [5], where the yield function is based on the yield locus description. The prediction of forming limits in [5, 6] has shown a strong influence of the shape of the yield function relating the plane strain and equi-biaxial stress states.

The aim of this paper is to describe the Vegter model implementation for the explicit FE code and the procedure of measurement of the most critical input material data required for numerical simulations of the AW 5754 aluminum alloy. Such measurements comprise the experimental results of not only static tensile tests, but also of hydraulic bulge tests, in order to determine the so-called biaxial point and biaxial anisotropy in the Vegter model, respectively. The results of numerical simulation are compared with those obtained using the conventional Hill 48 yield criterion [7], which is still frequently used in case of the material input data lack.

**Experimental Procedure.** In this work, an AW 5754 H11 aluminum alloy, which is widely applied in the automotive industry for production of inner body parts, was used (as a sheet material of 0.8 mm thickness). Its chemical composition being shown in Table 1, this alloy has a medium strength, is age-hardened and can not be heat-treated.

Since aluminum alloys are characterized by a high anisotropy, their behavior has to be described in the FEM code within framework of the advanced material model. Elaboration

of advanced material models like the Vegter or Barlat ones requires the conduction of numerous basic mechanical tests. The Vegter model was developed, in order to obtain a high accuracy combined with a simple mathematical description and a large flexibility. The original Vegter model uses the experimental results from from nine types of tests. In order to reduce the number of parameters in the model, a new variant, the so-called Vegter lite model has been developed [6]. Actually, only two test types are required for construction of the Vegter yield function, the first one being the static tensile test and the second one – the hydraulic bulge test, which is required for finding position of the biaxial stress  $\sigma_{biaxial}$  point.

Static tensile tests were carried out using an universal testing machine TiraTEST 2300, which is a microprocessor-controlled machine for strength tests with the maximum test load of 100 kN and measuring ranges of 1, 10, and 100 kN. Specimens used in this test were cut in three directions (0, 45, and 90°) related to rolling direction. The basic mechanical properties with planar anisotropy are shown in Table 2.

T a b l e 1

**Chemical Composition of Aluminum Alloy AW 5754 H11 (wt.%)**

Mg	Mn+Cr	Mn	Si	Fe	Cr	Zn	Ti	Cu	Other
3.60	0.60	0.50	0.40	0.40	0.30	0.20	0.15	0.10	0.15

T a b l e 2

**Basic Mechanical Properties of AW 5754 H11**

Direction (deg)	$R_e$ , MPa	$R_m$ , MPa	$A_{80}$ , %	$r$	$r_m$	$\Delta r$	$n$	$n_m$	$\Delta n$
0	115	231	19.6	0.655	0.797	-0.214	0.282	0.283	-0.0002
45	112	220	26.1	0.904			0.283		
90	116	221	25.4	0.723			0.283		

The hydraulic bulge test is a method to test a sheet metal under the equibiaxial stress state. A sheet metal specimen is clamped between blankholder and die while it is subjected to increasing fluid pressure as it is shown in Fig. 1. As the sheet specimen bulges, the region near the pole of bulge becomes almost spherical. This test is used to identify a very important point on the yield curve, which determines the yield stress at the equibiaxial stress state.

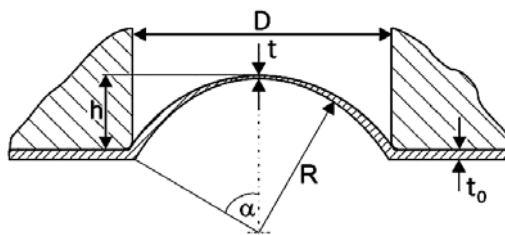


Fig. 1. Schematic of the hydraulic bulge test.

Due to the stress state observed in this case being different from that in the static tensile test, for construction of its stress–strain curve it is necessary to calculate the

so-called effective stress  $\sigma_i$  and effective strain  $\varphi_i$ . The respective values are derived from Eqs. (1)–(3), as follows

$$\sigma_i = \frac{pR}{2t}, \quad (1)$$

$$t = t_0 \left( \frac{\sin \alpha}{\alpha} \right)^2, \quad (2)$$

$$\varphi_i = -\varphi_3 = -\ln(t/t_0), \quad (3)$$

where  $\sigma_i$  is effective stress (MPa),  $p$  is pressure (MPa),  $\varphi_i$  is effective strain,  $R$  is the radius of curvature (mm), and  $t$  and  $t_0$  are the actual and initial thickness values (mm), respectively.

During the test, the pressure and the actual height of dome are measured. Using Eqs. (1)–(3) the stress–strain curve can be constructed. Comparison of stress–strain curves based on the uniaxial tensile and hydraulic bulge tests is shown in Fig. 2. The test sequence was recorded using ARAMIS system to measure strain distribution and determine the biaxial coefficient  $r_{biaxial}$ .

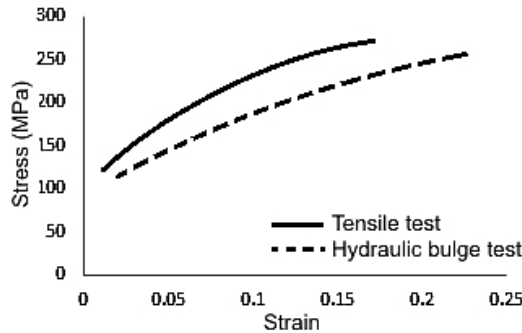


Fig. 2. Comparison of stress–strain curves from uniaxial tensile and hydraulic bulge tests.

Based on these calculated results, it was necessary to create a material model in the simulation software (Fig. 3) that accurately describes the behavior of the sheet material. Numerical simulations of Swift drawing test were carried out with the PAM-STAMP 2G software for prediction of metal forming processes. This FEM code offers numerous combinations of different hardening laws and yield functions. In this work, two different yield functions were evaluated in combination with the Krupkowski hardening law, which implies two regions of deformation. In the first region, the hardening effect exceeds the thickness reduction effect. The second area is characterized by the condition that hardening can not be compensated by the reduction of tractive force due to reduction of thickness. The Krupkowski formula can be expressed by the following equation:

$$\sigma = K(\varepsilon_0 + \varepsilon_p)^n, \quad (4)$$

where  $\varepsilon_p$  is plastic strain,  $\varepsilon_0$  is offset strain,  $n$  is strain-hardening exponent, and  $K$  is the material constant. Parameters for the Krupkowski law in the direction parallel to the rolling direction were fitted and set to  $K = 0.3481$  GPa,  $n = 0.137$ ,  $\varepsilon_0 = 0.00032$ . The value of  $r_{biaxial}$  was determined from the hydraulic bulge test. Parameters of the Krupkowski law were obtained from the uniaxial tensile test and processed in Excel.

The yield function can describe plastic behavior of a sheet material in the multiaxial stress state. As it was mentioned above, two yield functions were applied to compare the accuracy of the material model. For aluminum alloys, the Vegter model should be more suitable due to more convenient results. Simulation results were compared with those obtained via the Hill 48 model [7], because this yield function is still one of most commonly used material models in numerical simulations. The material data required for defining the yield function are shown in Fig. 3.

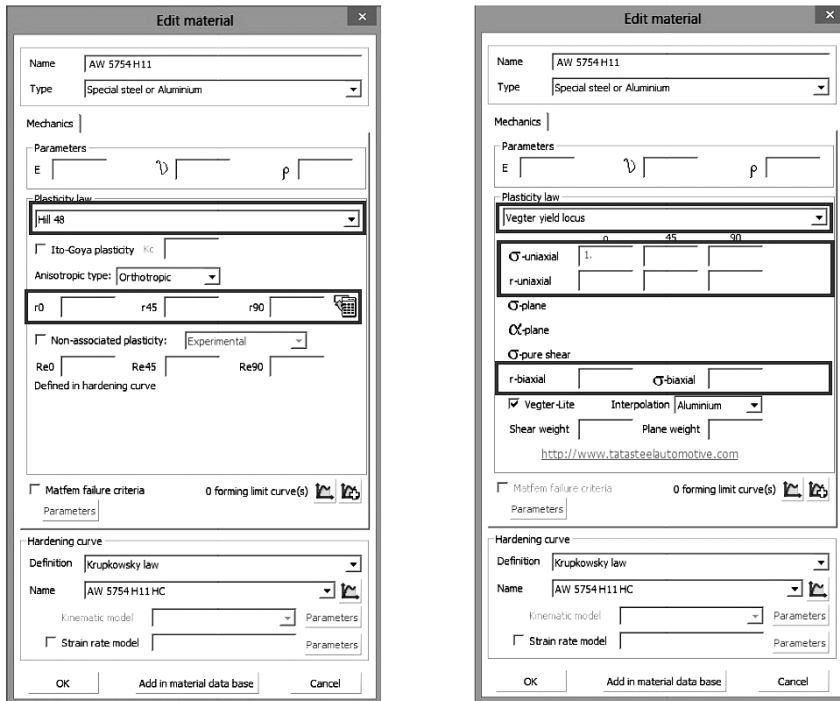


Fig. 3. The material data required for both applied yield functions.

In 1948, Hill introduced the concept of material anisotropy into the yield function equations for the first time [7]. According to the Hill yield function, in case of uniaxial stress state, the local thickness reduction occurs along the most vulnerable direction, which is the loading direction. Hill assumed that the direction of thickness reduction is compliant with the direction of zero extension, and therefore the deformation of narrowed areas appears only as reduction in thickness. Hill 48 is one of the most commonly used material model for conventional steel sheets. This yield function is set to be used with isotropic hardening law. The yield function was proposed for orthotropic materials. Based on the von Mises yield function, Hill has created a reasonable mathematical model to describe the anisotropic plastic flow. The latter led to establishment of the theory of anisotropic plastic deformation,

$$F(\sigma_{yy} - \sigma_{zz})^2 + G(\sigma_{zz} - \sigma_{xx})^2 + H(\sigma_{xx} - \sigma_{yy})^2 + 2L\sigma_{yz}^2 + 2M\sigma_{zx}^2 + 2N\sigma_{xy}^2 = 1. \quad (5)$$

In the above formula,  $x, y, z$  are the orthotropic axes. Parameters  $F, G, H, L, M,$  and  $N$  are the independent anisotropic characteristic parameters determined by experiments for different materials. In the numerical simulation, a simplified quadratic yield function corresponding to the planar anisotropic and normal anisotropies is used:

$$\sigma_Y^2 - \frac{2r}{1+r} \sigma_1 \sigma_2 + \sigma_2^2 = \sigma_Y^2, \quad (6)$$

where  $\sigma_Y$  is the yield stress and  $r$  is the Lankford coefficient of normal anisotropy.

The Vegter criterion provides a possibility of a more accurate description of the yield locus by a series of experimental points. Vegter was able to establish a first quadrant of the yield function using the points obtained from the basic experimental measurements. The Bezier interpolation is performed between points to construct the ellipses. Each point must have 3 parameters (two main stresses  $\sigma_1$ ,  $\sigma_2$  and strain vector  $\rho = d\varepsilon_2/d\varepsilon_1$ ). In order to describe a planar anisotropy by this model, it is necessary to have 17 parameters from 9 mechanical tests. Figure 4 illustrates the requirements for the conventional and lite Vegter material models. Mathematical expression of this yield function is as follows:

$$\begin{pmatrix} \sigma_1 \\ \sigma_2 \end{pmatrix} = (1-\lambda)^2 \begin{pmatrix} \sigma_1 \\ \sigma_2 \end{pmatrix}_i + 2\lambda(1-\lambda) \begin{pmatrix} \sigma_1 \\ \sigma_2 \end{pmatrix}_i^h + \lambda^2 \begin{pmatrix} \sigma_1 \\ \sigma_2 \end{pmatrix}_{i+1}, \quad (7)$$

where  $\lambda$  is the parameter for the Bezier interpolation.

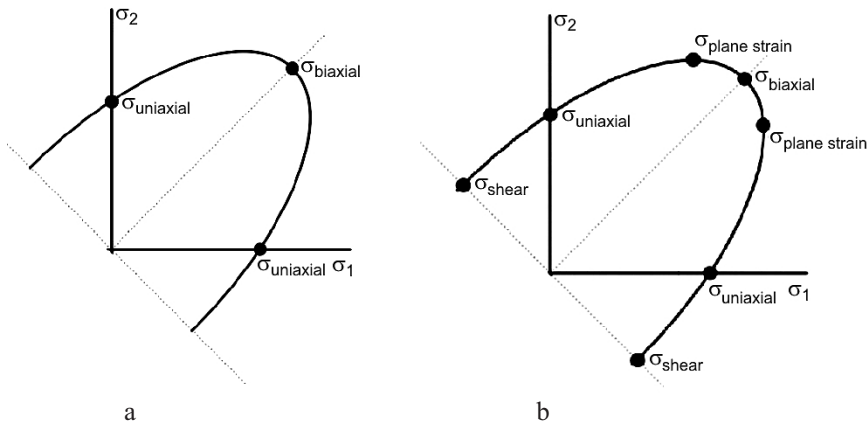


Fig. 4. The Vegter lite model (a) with NURBS interpolation and the Vegter yield locus (b) with the Bezier interpolation between points.

There is a possibility to use a simplified (the so-called Vegter lite formula). It is an optional model that uses only 7 parameters instead of 17 by skipping plane strain and pure shear information. To define this 7 parameters, only 3 mechanical tests are needed, including the static tensile test, hydraulic bulge test and measurements of the anisotropy ( $\sigma_{uniaxial}^{45^\circ}$ ,  $\sigma_{uniaxial}^{90^\circ}$ ,  $\sigma_{biaxial}$ ,  $r_{uniaxial}^{0^\circ}$ ,  $r_{uniaxial}^{45^\circ}$ ,  $r_{uniaxial}^{90^\circ}$ , and  $r_{biaxial}$ ). From the static tensile and hydraulic bulge tests, the reference points  $\sigma_{uniaxial}$ ,  $\sigma_{biaxial}$  are determined, which is shown in Fig. 5a. Then, using the planar anisotropy data, points normal to reference points are constructed (Fig. 5b). After this, these points are used to derive tangents to the Vegter lite model. Using the Bezier interpolation between reference points (Fig. 5c), the hinge points (as intersections points from the known slope in these reference points) are also identified.

For the purpose of verifying the accuracy of used yield functions, the deep drawing cupping test was carried out in explicit dynamic finite element code. In the numerical simulation, the tools were assumed to be rigid and the blank was elastic-plastic. We used the die with inner diameter of 52.5 mm and radius of 2.5 mm. The punch diameter of 50 mm

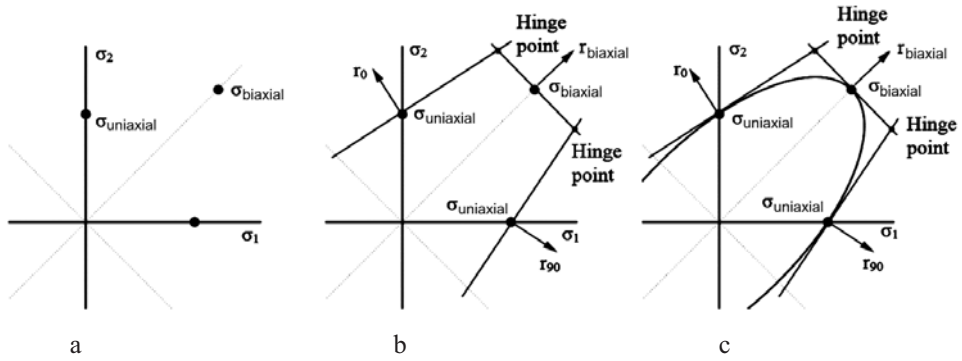


Fig. 5. The Bezier interpolation between the reference points for the Vegter lite material model.

and radius of 5 mm was assumed. The blankholder force is approximated to be 8 kN. The friction coefficient was 0.12 mm, which simulated the conditions similar to drawing with lubrication. In the numerical simulation, the shell mesh type was used with mesh size of 5 mm. Mesh size after final refinement was 1.25 mm. During the deep drawing simulation, the circular blank was clamped between blankholder and die, and then the punch was shifted down until the assigned stroke was reached. Positioning of the forming tool and blank before drawing process is shown in Fig. 6. Comparison of several yield criteria for AW 5754 H11 alloy, which can be set in simulation FEM code as shown in Fig. 7.

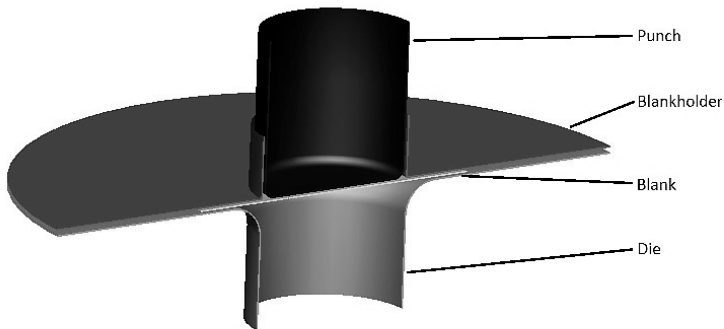


Fig. 6. Rapid drawing cup test.

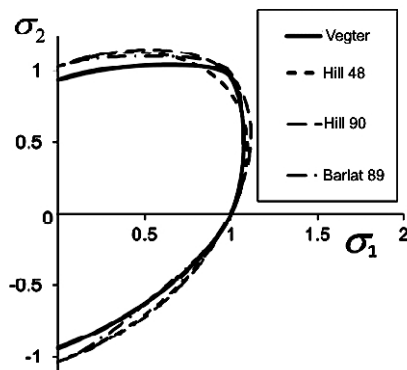


Fig. 7. Comparison of yield functions for AW 5754 aluminum alloy.

**Results and Discussion.** For numerical simulation simple drawing of axisymmetric cup with the diameter of 50 mm was chosen. In order to achieve the formability limits, the initial blank diameter was 90 mm, which indicates the computational model influence on the forming limit strains. For a contact between the tool and the formed sheet, the friction coefficient of 0.12 was selected, while the blank holding force was set to 8 kN.

A significant difference between the results using the Vegter lite and the Hill 48 yield models was observed. As seen from Fig. 8, large differences in the limit strains were observed. During the simulation, crack initialization with the Hill 48 yield function for the transition between the bottom and wall of the cup occurs (see Figs. 8a and 9a), while within the Vegter lite model the crack did not appear, as shown in Figs. 8b and 9b. The true experiments of stamping under the same technological conditions as used in simulation were performed. The Vegter lite results show a good agreement with the true drawn cup (Figs. 10 and 11), but the results obtained by the Hill 48 function are different. On the basis of the performed measurements and experiments, it is possible to conclude that the computational Vegter lite model is much more suitable for special alloys and zones with high deformation than model Hill 48. A similar conclusion has been reached by other researchers [8, 9].

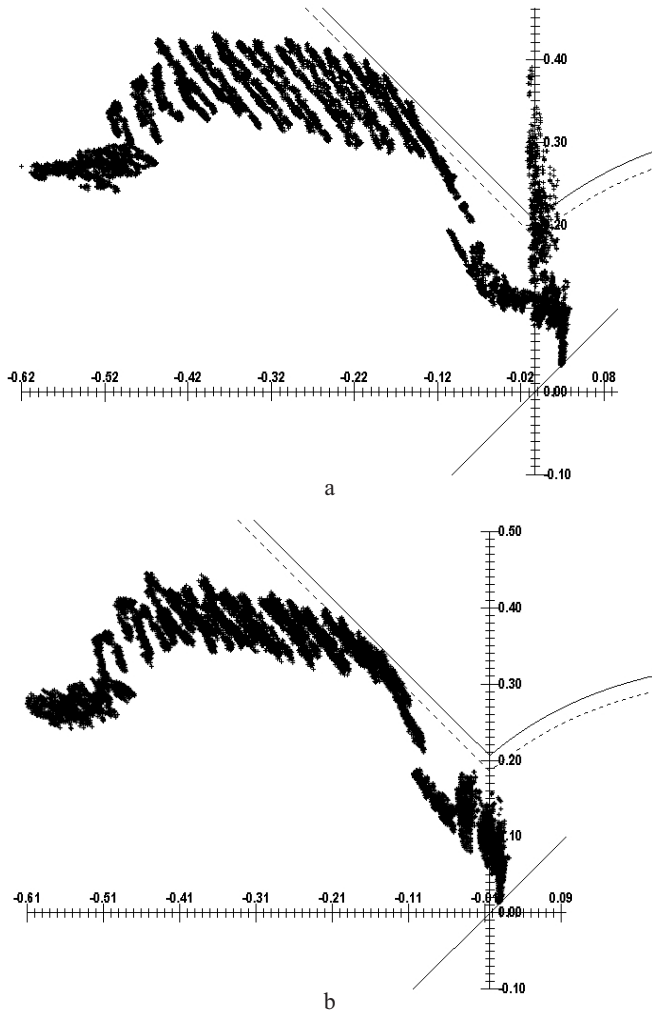


Fig. 8. Comparison of the FLDs from numerical simulation for the Hill 48 (a) and the Vegter lite (b) anisotropic yield criteria.

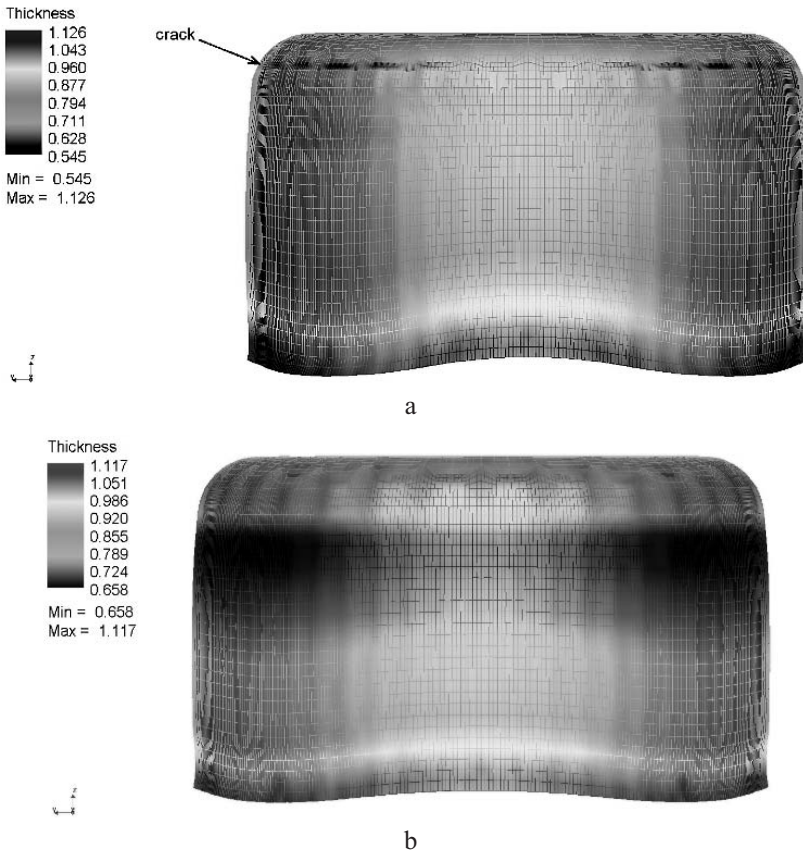


Fig. 9. Comparison of predicted thicknesses for the Hill 48 (a) and the Vegter lite (b) anisotropic yield functions.



Fig. 10. A final drawn cup with no crack.

**Conclusions.** The influence of advanced material model on numerical simulation results was evaluated. Predictive numerical simulations of deep drawing of a simple axisymmetric cup of the anisotropic aluminum alloy AW 5754 were carried out. The material model with the Hill 48 yield function was compared with the Vegter lite criterion. The true cups under the same technological conditions as used in predictions were deep drawn. Accurate forming simulations require accurate material models. The Vegter lite yield function, due to its more complex description of material, offers more accurate results. In FEM implementation, the CPU time was comparable to those of the Hill 48 model.

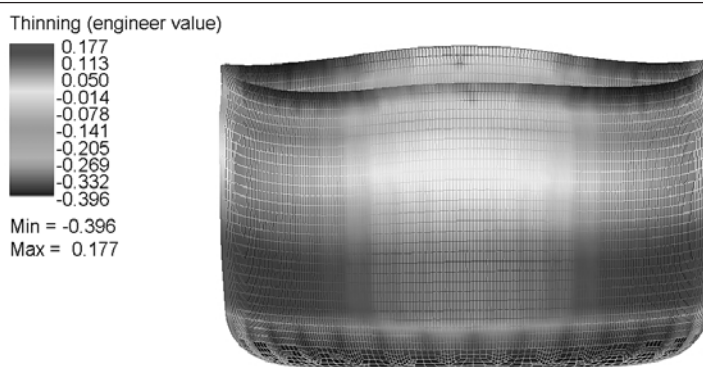


Fig. 11. Thinning at the punch stroke edge.

**Acknowledgments.** The authors gratefully acknowledge the financial support of the project VEGA 1/0872/14.

1. S. Bruschi, T. Altan, D. Banabic, et al., “Testing and modelling of material behavior and formability in sheet metal forming,” *CIRP Ann.-Manuf. Techn.*, **63**, Issue 2, 727–749 (2014).
2. F. Barlat, H. Aretz, J. W. Yoon, et al., “Linear transformation-based anisotropic yield functions,” *Int. J. Plasticity*, **21**, 1009–1039 (2005).
3. D. Banabic, T. Kuwabara, T. Balan, and D. S. Comsa, “An anisotropic yield criterion for sheet metals,” *J. Mater. Process. Technol.*, **157-158**, 462–465 (2004).
4. D. Banabic, D. S. Comsa, M. Sester, et al., “Influence of constitutive equations on the accuracy of prediction in sheet metal forming simulation,” in: P. Hora (Ed.), Proc. of 7th Int. Conf. (NUMISHEET 2008, Sept. 1–5, 2008, Interlaken, Switzerland) (2008), pp. 37–42.
5. H. Vegter and A. H. Boogaard, “A plane stress yield function for anisotropic sheet material by interpolation of biaxial stress states,” *Int. J. Plasticity*, **22**, 557–580 (2006).
6. H. Vegter, C. ten Horn, and M. Abspoel, “The Corus–Vegter lite material model: simplifying advanced material modelling,” *Int. J. Mater. Forming*, **2**, No. 1, 511–514 (2009).
7. R. Hill, “A theory of the yielding and plastic flow of anisotropic metals,” *Proc. Roy. Soc. Lond. A Math. Phys. Sci.*, **193**, Issue 1033, 281–297 (1948).
8. P. Solfronk, J. Sobotka, M. Kolnerova, and L. Zuzanek, “Utilization of advanced computational models for drawing process numerical simulation of titanium alloy,” in: Proc. of 24th Int. Conf. on Metallurgy and Materials: Metal 2015 (June 3–5, 2015, Brno, Czech Republic), pp. 1–6.
9. J. Novy, V. Vache, and J. Sobotka, “Influence of used yield function in deep drawing simulation of highly anisotropic aluminum alloy,” in: Proc. of Int. Conf. IDDRG 2013 (June 2–5, 2013, Zurich, Switzerland), pp. 273–277.

Received 10. 08. 2016